Macroscopic mid-FTIR mapping and clustering-based automated data-reduction : an advanced diagnostic tool for in situ investigations of artworks

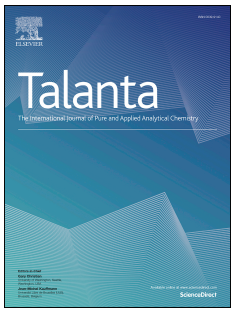

Macroscopic mid-FTIR mapping and clustering-based automated data-reduction: An advanced diagnostic tool for in situ investigations of artworks

Giorgia Sciutto, Stijn Legrand, Emilio Catelli, Silvia Prati, Cristina Malegori, Paolo Oliveri, Koen Janssens, Rocco Mazzeo

PII: S0039-9140(19)31208-1

DOI: https://doi.org/10.1016/j.talanta.2019.120575

Reference: TAL 120575

To appear in: *Talanta*

Received Date: 3 July 2019

Revised Date: 14 November 2019

Accepted Date: 18 November 2019

Please cite this article as: G. Sciutto, S. Legrand, E. Catelli, S. Prati, C. Malegori, P. Oliveri, K. Janssens, R. Mazzeo, Macroscopic mid-FTIR mapping and clustering-based automated data-reduction: An advanced diagnostic tool for in situ investigations of artworks, *Talanta* (2019), doi: https://doi.org/10.1016/j.talanta.2019.120575.

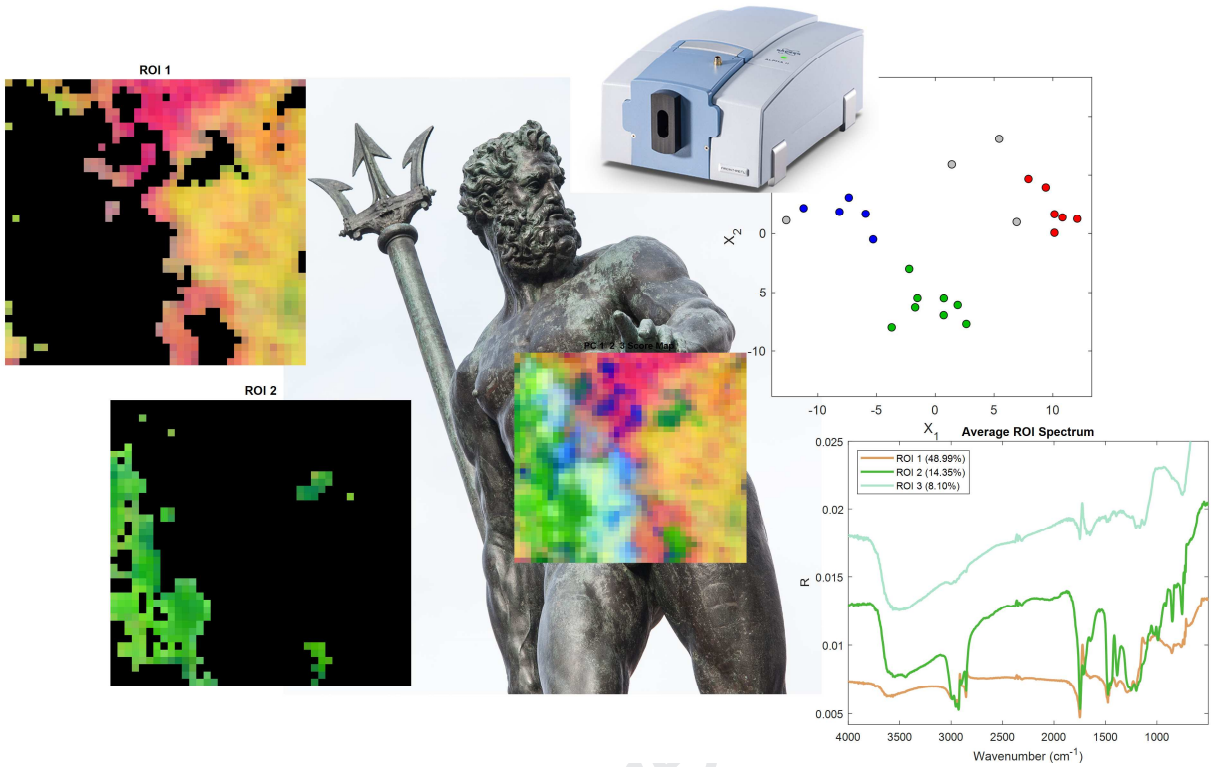
ROI 1
ROI 2
PC1, 2, 3 Score Map
X2
X1
Average ROI Spectrum
ROI 1 (48.99%)
ROI 2 (14.35%)
ROI 3 (8.10%)
R
Wavenumber (cm-1)

MACROSCOPIC MID-FTIR MAPPING AND CLUSTERING-BASED AUTOMATED DATA-REDUCTION: AN ADVANCED DIAGNOSTIC TOOL FOR IN SITU INVESTIGATIONS OF ARTWORKS

Giorgia Sciutto[1], Stijn Legrand[2], Emilio Catelli[1], Silvia Prati[1], Cristina Malegori[3], Paolo Oliveri[3,*], Koen Janssens[2,**], Rocco Mazzeo[1]

[1]University of Bologna, Dept. of Chemistry "G. Ciamician", Ravenna Campus, Via Guaccimanni 42 – 48100 Ravenna, Italy

[2]University of Antwerp, Dept. of Chemistry, Campus Groenenborger, Groenenborgerlaan 171 – 2020 Antwerp, Belgium

[3]University of Genova, Dept. of Pharmacy (DIFAR), Viale Cembrano 4 – 16148 Genova, Italy

Abstract

The present study describes a multivariate strategy that can be used for automatic on-site processing of reflection mode macro FTIR mapping (MA-rFTIR) data obtained during investigation of artworks. The chemometric strategy is based on the integration of principal component analysis (PCA) with a clustering approach in the space subtended by the three lowest-order principal components and allows to automatically identify the regions of interest (ROIs) of the area scanned and to extract the average FTIR spectra related to each ROI. Thanks to the automatic data management, in-field HSI (hyperspectral imaging)-based analyses may be performed even by staff lacking specific advanced chemometric expertise, as it is sometimes the case for conservation scientists or conservators with a scientific background. MA-rFTIR was only recently introduced in the conservation field and, in this work the technique was employed to characterize the surface of metallic artefacts. The analytical protocol was employed as part of a rapid procedure to evaluate the conservation state and the performance of cleaning methods on bronze objects. Both activities are commonly part of restoration campaigns of bronzes and require an on-site analytical procedure for efficient and effective diagnosis. The performance of the method was first evaluated on aged standard samples (bronzes with a layer of green basic hydroxysulphate, treated with different organic coatings) and then scrutinized in situ on areas of the 16th century Neptune fountain statue (Piazza Duomo, Bologna, Italy) by Gianbologna.

Keywords

Automatic multivariate strategy; Hyperspectral imaging-based analyses; Macroscopic Mid-Infrared mapping; Cluster analysis; Principal Component Analysis; Bronze objects.

1. Introduction

Non-invasive techniques are essential tools for analysis in the field of conservation, because they preserve the integrity of the artwork and allow an extensive documentation of its surface to be acquired. Several miniaturized devices have been developed that allow for in situ examinations. In this way, the risks and costs related to handling artworks are reduced. Spectroscopic hyperspectral-based analyses allow for easy and extensive investigations on the surface of an object, providing the possibility to obtain chemical images related to the distribution of a single molecular species/moiety or of a single chemical element. Data acquisition can be carried out by full field or pencil-beam imaging methods, which produce, in both cases, a 3D data matrix [1]. This 3D data matrix contains the spatial information in two (x and y) dimensions, while the spectral information is present in the

third (z) dimension. To date, macroscopic X-ray fluorescence scanning (MA-XRF) [2, 3] and visible-near infrared (VNIR) or short-wave infrared (SWIR) devices are the most widely used hyperspectral instruments for the in-situ analysis of paintings [4, 5] and illuminated manuscripts [6, 7]. The use of the mid infrared (MIR) spectral region for macroscopic imaging or mapping analysis in the reflection mode (MA-rFTIR) represents a quite attractive but poorly explored approach, due to limitations concerning instrument costs. The imaging systems so far proposed for the analysis of paintings [8, 9] operates in a reduced spectral subregion of MIR: 900-1400 cm^{-1} [8] and 3700-1800 cm^{-1} [9]. Additionally, a low-noise MIR imaging spectrometer operating in the region 1240-760 cm^{-1} for fast acquisition of paintings has been presented [10]. The high cost of these instruments, together with the limit in terms of detectable spectral range, make a wide application in museums or private laboratories prohibitive. As a powerful alternative to avoid the use of an expensive focal plane array (FPA) detector, an in-house portable point-scan FTIR spectrometer mounted on a motorized 3D stage has been recently proposed for the mapping of chemical species on paintings. This compact and cost-effective spectrometer has also the advantage to cover the entire MIR range and a portion of the NIR range (7500-375 cm^{-1}) [11, 12].

In the present research, an innovative chemometric strategy was developed to improve the processing of hyperspectral data. The automated approach proposed allows to reduce the time required for data processing. By maximizing the degree of automation of the procedure, data analysis is rendered easier and becomes more directly applicable by personnel that does not have advanced chemometric insights; often, such is the case for conservation scientists or conservators. The strategy allows to automatically identify (sub)regions of interest (ROIs) in the area scanned, after application of principal component analysis (PCA) on the FITR spectral 3D data matrix. In a second phase, the PC score maps are automatically clustered by the density-based spatial clustering of applications with noise (DBSCAN) algorithm [13]. In the present study, the DBSCAN algorithm was integrated with PCA for the processing of hyperspectral data. The DBSCAN algorithm presented peculiar advantages, compared with other clustering algorithms: (i) minimal requirements of domain knowledge to determine the input parameter, (ii) identification of clusters of irregular shape, (iii) good efficiency on large databases. Most important, DBSCAN does not require neither the a-priori definition of the number of clusters nor a decisional intervention by the operator. This allowed a more efficient extraction of information, in an automatic way, which was the purpose of the strategy proposed. In this manner, for each ROI, the corresponding average FTIR spectrum is obtained. Evaluation of the spectral profiles can then be performed to achieve a better understanding of the chemical variability within the selected area. With a single-step approach, the automatic algorithm allows to obtain: (i) the proper selection of the most representative areas (in terms of spectral information and number of pixels), (ii) the automatic extraction of the most significant spectra from all the investigated areas.

PCA-based chemometrics approaches coupled with MIR spectroscopy have already been proposed for the investigation of micro cross-sections of paintings [14, 15]. Different statistical methods have been also presented for the data management and reduction of reflectance image-cubes obtained in visible – near infrared (V-NIR) and short-wave infrared (SWIR) ranges. Among others, methods that enable the identification and mapping of most representative spectra ("endmembers") in the data-cube are well established in the field of cultural heritage. In particular, methods based on the use of the so-called hourglass paradigm (ENVI software, Harris Corporation, Melbourne, FL, USA) to extract the endmembers and combined with the spectral angle-mapping (SAM) algorithm, to visualize the pigment distributions, have been successfully employed for the study of illuminated manuscripts and paintings [4, 5]. Nevertheless, the complexity of these chemometric data

processing requires a deep expertise in multivariate analysis and a lot of super-vised/manual interpretation efforts [16]. These requirements are not always compatible with on-site diagnostic campaigns and cannot guarantee that the results will be obtained in real time.

The chemometric strategy here presented was developed to quickly and easily obtain chemical information from complex dataset. In particular, application of MA-rFTIR mapping analysis on metal patinas is described. The results provide information on the state of conservation to support the on-site development of appropriate conservation treatments, during ongoing restoration campaigns. Indeed, although MA-FTIR systems usually required a long acquisition time for the analysis of rather small areas, the application of a fast data processing method may help in reducing the overall investigation time.

Recently, in-situ hyperspectral imaging in the short-wave infrared (SWIR) region was successfully used to map two bronze corrosion products, brochantite and antlerite, on the surface of the outdoor bronze sculpture the "Man with the Key" by Auguste Rodin in Oslo [17]. In that study, two areas of the corroded bronze were analyzed and data were successively processed by an "ad hoc" multivariate approach based on singular value decomposition (SVD), iterative key set factor analysis (IKSFA) and spectral angle mapping (SAM). The approach first seeks and extracts the purest spectra from the 3D data cube (SVD and IKSFA). Successively, by means of overtones and combination bands, the purest spectra are assigned to a pertinent corrosion product. Spatial distribution of the identified corrosion compounds is eventually obtained by the SAM algorithm. Although combination bands and higher overtones of fundamental vibrations proved to be useful in the identification of corrosion products, they suffer from lower selectivity in comparison to the bands in the fingerprint MIR range, with the risk of loss of important information.

Here, the proposed analytical protocol was tested as a time-efficient manner of evaluating the conservation state of bronze objects, by identifying both corrosion products and coatings and exploiting the diagnostic and selective character of mid-IR range, and the performance of associated cleaning methods. These two activities are commonly part of restoration campaigns and need to be supported in real time with an easy and suitable analytical procedure. The MA-rFTIR approach combined with automated data elaboration proved to be efficient in showing the distribution of organic treatment residuals as well as the presence of the corrosion product brochantite. The distribution maps obtained can clearly offer a valid help to restorers in taking important decision on the restoration of the sculpture. The information acquired is meaningful and the millimeter-size spatial resolution, low compared to a SWIR-NIR hyperspectral camera, does not highly affect the information that can be extracted.

Subsequently, analysis of MA-rFTIR data obtained from standard copper coupons, with a green basic copper hydroxysulfate (brochantite) patina and different protective coatings, is discussed. After that, the application of the data reduction procedure to hyperspectral maps obtained from the 16th century Neptune fountain in Bologna, Italy, and collected in situ during the last restoration campaign in 2016, is described. The first aim of the latter investigation was to understand and document the state of conservation of the bronze surface by considering the distribution of corrosion products and the presence of residual treatment compounds applied during the all-but-last restoration in 1989-1990 [18]. As a second goal, the suitability of the MA-rFTIR system for in situ monitoring of the efficacy of cleaning procedures aimed at removing deteriorated coatings from the metal surface was evaluated.

2. Materials and Methods

2.1 Samples

Two copper plates (5 x 7 cm), named R6 and R57, were selected as test samples (Figures 1.a and 1.b). The copper substrate is covered by a thin layer of brochantite ($Cu_4SO_4(OH)_6$) formed naturally by exposure to the urban atmosphere of Munich (Germany) for almost 80 years. Each sample has been divided in three equally-sized rectangular areas of dimension 1.6 x 7.0 cm. The first area, denoted with letter B was untreated with plain brochantite as a reference; the second area, denoted as I, was covered with a protective layer of Incralac, an acrylic resin-based formulation; the third area, denoted as W was treated first with Incralac and, successively, with a layer of microcrystalline wax. R6 was prepared in 2005 and exposed for 8 months in the urban atmosphere of Venice [19]. R57 was prepared in 2011 but never exposed to the outside atmosphere. The two coupons were preserved over the years in a controlled indoor laboratory environment. Incralac and microcrystalline wax R21 were purchased from Phase Srl (Bologna, Italy). The real case under examination was the famous renaissance bronze sculpture of Neptune by the sculptor Gianbologna, situated in Piazza del Nettuno, Bologna, Italy.

2.2 FTIR macro mapping

MA-rFTIR scans were performed, using an in-house portable point-scan FTIR spectrometer mounted on a motorized 3D stage [11]. The core of the instrument is an Alpha FTIR spectrometer (Bruker, Billerica, MA, USA), equipped with a frontal reflectance module (20°/20° geometry), controlled by OPUS 6.0 software (Bruker, Billerica, MA, USA). The spectra were acquired in reflection mode in the range 375-7500 cm^{-1} with a spectral resolution of 4 cm^{-1}. The spectrometer is positioned during the scan on a 100 x 250 x 100 mm^3 motion system (Newport Corporation, Irvine, CA, USA). X and Y stages are employed for the actual scanning motion, while the Z stage is used to bring the XY scanning plane parallel to the object under investigation. Prior to each scan, a background measurement of 15 minutes was performed to compensate for infrared-absorbing compounds in the environment atmosphere. Approximately 10 min was necessary to position the instrument probe-head in front of the sample to be analyzed, at 1.5 cm distance. The copper plates were analyzed by scanning an area of 50.5 x 35.5 mm^2 on sample R57 and 51.5 x 33 mm^2 on sample R6, with the acquisition time per pixel of 3s, following a 0.5 x 0.5 mm^2 grid. The acquisition time of each area was approximately 15 hours. Regarding the scanning of the Neptune sculpture, the acquisition time per pixel was 3s, using a 1 x 1 mm^2 grid. The analyzed areas have dimension 42 x 40 mm^2 and 22 x 22 mm^2; the acquisition time was 4 hours for the first area and 1 hour and 10 minutes for the second area.

2.3 Data processing

Three-dimensional data arrays corresponding to hyperspectral maps were preliminarily unfolded to two-dimensional data matrices, in which the rows correspond to pixels while the columns refer to spectral variables, to allow direct processing by means of principal component analysis (PCA). The unfolded 2D matrices were pre-processed by means of the standard normal variate (SNV) transform [20, 21] to correct for undesired physical variations within spectra, and by column mean-centering. PCA was then applied, resulting in a score matrix, with as many rows as the pixels of the map and as many columns as the principal components (PCs) retained [22]. Score values (i.e. the magnitude of the various PCs in each pixel) were used to construct a composite score map as a false-color image in which the red, green and blue channels are encoded by the PC1, PC2 and PC3 score values, respectively, under the assumption that the three lowest-order PCs embody the most relevant information. This is reasonable for highly inter-correlated variables, such as spectral ones. Score values were preliminarily scaled between 0 and 255 in each channel. This type of combined

maps allows to efficiently identify areas characterized by different score values and, thus, by a different spectral response thanks to their different colors. To recognize the regions of interest (ROIs, a specific spatial region identified within the analyzed area) in an automated manner, the density-based spatial clustering of applications with noise (DBSCAN) algorithm [13] was applied, using PC1-to-PC3 scaled score values as the input variables and pixels as the objects to be clustered. The DBSCAN algorithm identifies groupings of pixels that have similar sets of scores and, therefore, similar false colors in the composite map. Other clustering approaches were previously used for automated clustering of spectral data in a reduced PCA space [23]. DBSCAN identifies non-linearly separable clusters, defined as groupings of objects that are mutually close to each other within a high-density region in the multivariate space. Two parameters must be set: minPts (the minimum number of objects that may define a cluster) and ε (the maximum radius of the neighborhood from an object in which other objects are considered as belonging to the same cluster). In the present study, minPts was set equal to N/120, where N is the total number of pixels in the map, and ε was set equal to 19, from empirical evaluations. The choice of the clustering parameters has been optimized for this type of spectral data and the user does not have to change these settings while operating. These parameters can be, in fact, reasonably maintained constant for analyzing data of the same typology.

Clusters of pixels identified by DBSCAN, corresponding to relevant ROIs in the area mapped can be directly highlighted. Clustering is a necessary step in the proposed strategy, to automatically provide the operator with the chemical information (from the averaged spectrum) related to the regions of interest within the map. Simultaneously, the average spectral profile of the pixels constituting each ROI can be computed and plotted, with a color-coded indication of the correspondence ROI-spectrum. This combination of automatic identification of ROIs performed by DBSCAN – with ROI visualization on the map – and of the extraction of their average spectra constitutes a very efficient data reduction and exploration procedure, in which the intervention of the user is essentially unnecessary. Multivariate data processing and analysis of graphical outputs were performed by means of ad hoc in-house Matlab routines (The MathWorks, Inc., Natick, USA, Version 2018a).

3. Results and Discussion

3.1 Model bronze samples

The automatic chemometric processing developed for MIR macro mapping data was tested to quickly solve some diagnostic problems, which usually occurs during a restoration campaign on historical metal artefacts. Before defining the appropriate conservation strategy, it is relevant to identify the state of conservation of an artwork in terms of occurrence of degradation products and the distribution of previous coatings. These two points allow to decide whether it is necessary to remove any residual coatings applied during past treatments and to apply (one or more) new ones, and if the object must be treated with a corrosion inhibitor (for example, in case of active corrosion processes due to the presence of chlorides). These two restoration activities usually need to be supported by results of analytical investigations that can be performed relatively quickly on site, and at the same time/just prior to the actual restoration activities.

The new analytical method was first tested on model bronze samples R6 and R57, naturally aged in urban environments and treated with traditional protective coatings. For each copper plate, a scan area encompassing the three different regions was selected and mapped by MA-rFTIR (Figures 1.a

and S1.a). After the acquisition of the MIR chemical maps, the 3D data matrices were submitted to the automatic multivariate data processing. PCA combined with clustering allowed an automatic selection of characteristic ROIs in the mapped area.

From the 3D data matrix obtained from sample R57 (only exposed to indoor atmosphere), the automatic data analysis produced an RGB false color PC1,2,3 score map, in which three different ROIs were identified that could be associated with the three different regions of the sample (Figure 1.b). The use of the three lowest-order PCs allowed to guarantee a minimal intervention by technical operators. In fact, for data – such as spectroscopic ones – in which variables are highly inter-correlated, the most relevant information is usually concentrated in the first two or three PCs [24]. Nevertheless, this screening approach does not exclude the possibility of deepener investigations, exploring the higher-order PCs by using more conventional multivariate approaches.

Each ROI was visualized individually (Figure 1.d-f), to better assess its position. Subsequently, the average reflection-mode FTIR spectrum was extracted to chemically characterize the selected area, also thanks to the comparison with the spectral signatures of pure standard materials (Figure S2).. Figure S3 (Supplementary Material) shows the effect of the standard normal variate (SNV) transform applied on spectral profiles of sample R57. It can be easily observed how this transform (Figure S3.b) minimizes unwanted systematic effects present within the spectral profiles, such as baseline shift and global intensity amplification (Figure S3.a). ROI 1 (yellow area, Figure 1.d) shows a homogeneous distribution of brochantite. The extracted spectrum showed distorted bands induced by specular and/or diffuse reflection (Figure S1.a). The reststrahlen band at 1086 cm^{-1} and the bands between 3600 and 3400 cm^{-1} refer to SO_4^{2-} and O–H stretching modes, respectively. Several weak bands in the spectral region between 2500 and 1600 cm^{-1} are likely ascribable to overtone and combination bands, visible thanks to the diffuse reflection contribution [25]. ROI 2 labeled with a green color (Figure 1.e) is characterized by the presence of Incralac, owing to the strong derivative-like shaped band in the range 1770-1700 cm^{-1}, ascribable to the C=O stretching mode. C–H bending bands in the range 1340-1450 cm^{-1} were well recognizable together with the C–O stretching band at about 1140 cm^{-1} (Figure S1.b). Brochantite, which is present underneath Incralac, remains detectable due to the presence of a weak O–H stretching band up to 3500 cm^{-1}. ROI 3 (violet area, Figure 1.f) evidences the presence of wax applied over the Incralac layer. The so-called “double coating system” of bronze statues in Mediterranean countries is traditionally used to extend the lifetime of the protective coatings [26]. This is probably the mostly used coating system applied to protect surface of outdoor sculptures from corrosion. The spectrum extracted from ROI 3 is characterized by the vibrational modes typical of long-chained carbon compounds such as wax (Figure S1.c). Derivative-like shaped bands in the spectral range between 2820-2940 cm^{-1} refer to the C–H stretching modes, while the double bands at 715 and 727 cm^{-1} are ascribable to C–H bending (methylene rocking) and are indicative of the presence of long aliphatic chains [25]. The contribution of the ester C=O stretching mode (band with a derivative-like shape at 1737 cm^{-1}) is ascribable to the underlying synthetic resin.

In sample R6 (exposed to outdoor urban atmosphere for half a year), four different ROIs were identified by the algorithm (Figure 2). The green ROI 1 (Figure 2.c) is ascribable to brochantite, as confirmed by the average spectrum (data not shown). Brochantite is situated in area B and in those zones of area I where the Incralac layer was degraded/eroded during exposure. Both ROI 2 and ROI 3 (pink region, Figure 2.e and red-brown region, Figure 2.f, respectively) are located in the area treated with Incralac. The automatic plotting of the average spectra easily allowed a prompt comparison among the different clusters/ROIs. ROI 2 showed the presence of the acrylic diagnostic bands (Figure 1S.d), while the spectral profile obtained from ROI 3 revealed the co-presence of

brochantite and Incralac with a higher contribution of brochantite. In fact, intense and well-defined O–H stretching modes at 3560-3590 cm^{-1} were more intense, as well the reststrahlen band at 1083 cm^{-1}, if compared with the C–O stretching band of Incralac at 1140 cm^{-1}. The inhomogeneous distribution of Incralac resulted from the deterioration of this layer induced by aging. The yellow ROI 4 (Figure 2.g) is associated to the undamaged layer of wax (spectral data not shown). It can be concluded from the discussion above that the evaluation of the analytical procedure on standard samples allows to establish the potentialities of the protocol for the easy and quick identification of different compounds on a surface.

3.2 Neptune statue

The MA-rFTIR imaging protocol was then employed to obtain information on the state of conservation of the Bologna Neptune statue during its restoration campaign in 2016. These analyses were aimed at characterizing the type of degradation products present on the surface, and at documenting the permanence of the coatings applied in the previous restoration, which dates back to 1989-1990. The corroded surface of the sculpture was then covered with a protective double layer coating made of Incralac and microcrystalline wax. Figure 3.a shows an altered area located on the gluteus of the Neptune sculpture that was submitted to MA-rFTIR mapping. The PC1,2,3 score map (Figure 3.b) shows a heterogeneous situation that allowed to identify three different ROIs within the scanned area (Figure 3.d-f). The scanned area is mainly included in ROI 1 (Figure 3.d), whose averaged spectrum (Figure S4.a) shows the presence of a discontinuous layer of wax (bands at 2820 and 2940 cm^{-1} and at 715 and 727 cm^{-1}). Indeed, the intense carbonyl bands at about 1725 cm^{-1} and the band at 1140 cm^{-1} reveal the diffuse presence of Incralac. The derivative-like shape of the main absorption bands suggests a strong contribution of the specular components. This indicates that, in this area, the wax layer maintained its texture during time. On this basis, a limited spread of alteration products in this area can be assumed. The average spectrum (Figure S4.b) extracted from ROI 2 (green region, Figure 3.e) did not show any evident deformation of the bands. This suggests that the diffuse reflection components are predominant in this area, indicating a more irregular and degraded surface. MIR signals from both protective coatings (wax and Incralac) are still visible, although those from the synthetic resin appear to dominate the spectrum. This suggests that the external wax layer was partially degraded in this ROI. Moreover, the broad OH band at about 3500 cm^{-1} and the shoulder at about 1160 cm^{-1} may suggest the presence of traces of corrosion products such as copper hydroxyl sulfates (Figure S4.b). Associated with ROI 3 (light-blue region, Figure 3.f) is an averaged spectrum in which broad and weak bands are present, probably affected by diffuse reflection (Figure S4.c). This corresponds to a coarse, strongly corroded surface. Only few traces of Incralac are still visible (band around at 1730 cm^{-1}). Additionally, in spectrum S4.c it is possible to observe a broad band at 3500 cm^{-1} due to the OH stretching and a broad band at around 1000 cm^{-1} that might be tentatively assigned to the stretching modes of sulfates or silicates. The bands, however, are too broad to securely assign them to a defined inorganic compound, probably due to some effects of overlapping. Micro-destructive analysis performed with micro FTIR, revealed the presence in the patina of copper hydroxysulfates, gypsum and silicates [25], which might be possible candidates to explain these bands.

From the results reported above, it is possible to conclude that the MA-rFTIR imaging method allows to distinguish the subregions of the mapped area by locating intact coatings and partially degraded regions. To further assess the applicability of the method, MA-FTIR mapping in combination with the automatic pixel clustering was used to monitor the cleaning procedures that

were employed on the Neptune statue. Restoration protocols often include the removal of aged coatings to be re-placed with new treatment layers. A region cleaned with acetone was analyzed, comparing the results with a neighboring and untreated area (Figure 4.a). The automatic clustering applied on the hyperspectral map resulted in four spatial ROIs. ROI 1 and ROI 2 (Figures 4.d and 4.e) are in the uncleaned area and they can be differentiated by a different amount of wax, confirming the inhomogeneity of the coatings as previously described. In both regions, Incralac was well recognizable due to the derivative-like shape band of the carbonyl stretching at about 1730 cm^{-1}, while ROI 1 showed a higher contribution of wax with respect to ROI 2, due to the presence of bands at 2918-2845 cm^{-1} and at 731-721 cm^{-1} (data not shown). ROI 3 is ascribable to the tape used to limit the un-treated area (Figure 4.f) and ROI 4 corresponds the acetone-cleaned area (Figure 4.g). The average spectra of the cleaned area confirmed the total removal of wax and the drastic reduction of the thickness of the Incralac layer (Figure S2.d), which was still partially present. Thus, CH stretching and bending modes were no longer present in the average spectrum extracted from ROI 4, while the C-O modes were still recognizable. Additionally, a broad and intense band at 1006 cm^{-1}, together with a band at 912 cm^{-1}, suggested the presence of silicate-based components, probably ascribable to a local deposition of dust. From this last hyperspectral map, it can be concluded that MA-rFTIR in combination with the automated spectral clustering method, can provide conservators with on-site monitoring information on the efficacy of the coating removal interventions they are applying.

4. Conclusions

In the present study, a new on-site analytical approach for the rapid and simple processing of hyperspectral data cube is proposed, based on macroscopic reflection mode FTIR scanning analysis. The approach allows in real time for the sorting of complex spectra data sets into a limited number of sub areas of the mapped region, each characterized by a distinct average spectrum.

The system was tested both on naturally corroded mockup samples and on surface areas of the 16th century Neptune statue and allowed to obtain information related to the metal patina of the investigated bronze surfaces. The method was proposed for the characterization of coatings applied as protective agents.

Even if, in the last decades, the relevance of scientific analyses in the conservation field has been acknowledged, the related time and expertise required are often not bearable. The automated approach proposed in the present study allows to reduce the time required for data processing by maximizing the degree of automation of the procedure. Data analysis becomes applicable on site during diagnostic campaigns to quickly obtain information for the definition of proper conservation actions. Additionally, the approach can be also suitable for the processing of data obtained from forensic and environmental analytical measurements, which usually aim to achieve reliable results in the shortest time possible.

5. References

[1] S. Legrand, F. Vanmeert, G. Van der Snickt, M. Alfeld, W. De Nolf, J. Dik, K. Janssens, Examination of historical paintings by state-of-the-art hyperspectral imaging methods: From scanning infra-red spectroscopy to computed X-ray laminography, Heritage Science 2(1) (2014). https://doi.org/10.1186/2050-7445-2-13.

[2] A. Martins, J. Coddington, G. Snickt, B. Driel, C. McGlinchey, D. Dahlberg, K. Janssens, J. Dik, Jackson Pollock's Number 1A, 1948: A non-invasive study using macro-x-ray fluorescence mapping (MA-XRF) and multivariate curve resolution-alternating least squares (MCR-ALS) analysis, Heritage Science 4(1) (2016). https://doi.org/10.1186/s40494-016-0105-2.

[3] G. Sciutto, T. Frizzi, E. Catelli, N. Aresi, S. Prati, R. Alberti, R. Mazzeo, From macro to micro: An advanced macro X-ray fluorescence (MA-XRF) imaging approach for the study of painted surfaces, Microchem. J. 137 (2018) 277-284. https://doi.org/10.1016/J.MICROC.2017.11.003.

[4] J.K. Delaney, J.G. Zeibel, M. Thoury, R. Littleton, M. Palmer, K.M. Morales, E.R. De La Rie, A. Hoenigswald, Visible and infrared imaging spectroscopy of picasso's harlequin musician: Mapping and identification of artist materials in situ, Appl. Spectrosc. 64(6) (2010) 584-594.

[5] C. Cucci, J.K. Delaney, M. Picollo, Reflectance Hyperspectral Imaging for Investigation of Works of Art: Old Master Paintings and Illuminated Manuscripts, Acc. Chem. Res. 49(10) (2016) 2070-2079. https://doi.org/10.1021/acs.accounts.6b00048.

[6] P. Ricciardi, S. Legrand, G. Bertolotti, K. Janssens, Macro X-ray fluorescence (MA-XRF) scanning of illuminated manuscript fragments: Potentialities and challenges, Microchem. J. 124 (2016) 785-791. https://doi.org/10.1016/J.MICROC.2015.10.020.

[7] P. Ricciardi, J.K. Delaney, M. Facini, J.G. Zeibel, M. Picollo, S. Lomax, M. Loew, Near infrared reflectance imaging spectroscopy to map paint binders in situ on illuminated manuscripts, Angew. Chem. Int. Ed. 51(23) (2012) 5607-5610. https://doi.org/10.1002/anie.201200840.

[8] F. Rosi, C. Miliani, R. Braun, R. Harig, D. Sali, B.G. Brunetti, A. Sgamellotti, Noninvasive analysis of paintings by mid-infrared hyperspectral imaging, Angew. Chem. Int. Ed. 52(20) (2013) 5258-5261. https://doi.org/10.1002/ange.201209929.

[9] A. Daveri, S. Paziani, M. Marmion, H. Harju, A. Vidman, M. Azzarelli, M. Vagnini, New perspectives in the non-invasive, in situ identification of painting materials: The advanced MWIR hyperspectral imaging, TrAC Trends Anal. Chem. 98 (2018) 143-148. https://doi.org/10.1016/J.TRAC.2017.11.004.

[10] F. Gabrieli, K.A. Dooley, J.G. Zeibel, J.D. Howe, J.K. Delaney, Standoff Mid-Infrared Emissive Imaging Spectroscopy for Identification and Mapping of Materials in Polychrome Objects, Angew. Chem. Int. Ed. 57(25) (2018) 7341-7345. https://doi.org/10.1002/anie.201710192.

[11] S. Legrand, M. Alfeld, F. Vanmeert, W. De Nolf, K. Janssens, Macroscopic Fourier transform infrared scanning in reflection mode (MA-rFTIR), a new tool for chemical imaging of cultural heritage artefacts in the mid-infrared range, Analyst 139(10) (2014) 2489-2498. https://doi.org/10.1039/C3AN02094K.

[12] K. Janssens, S. Legrand, G. Van Der Snickt, F. Vanmeert, Virtual archaeology of altered paintings: Multiscale chemical imaging tools, Elements 12(1) (2016) 39-44. https://doi.org/10.2113/gselements.12.1.39.

[13] M. Ester, H.-P. Kriegel, J. Sander, X. Xu, A density-based algorithm for discovering clusters in large spatial databases with noise, Kdd, 1996, 226-231.

[14] G. Sciutto, P. Oliveri, S. Prati, M. Quaranta, S. Lanteri, R. Mazzeo, Analysis of paint cross-sections: A combined multivariate approach for the interpretation of μaTR-FTIR hyperspectral data arrays, Anal. Bioanal. Chem. 405(2-3) (2013) 625-633. https://doi.org/10.1007/s00216-011-5680-1.

[15] F. Rosi, A. Federici, B.G. Brunetti, A. Sgamellotti, S. Clementi, C. Miliani, Multivariate chemical mapping of pigments and binders in easel painting cross-sections by micro IR reflection spectroscopy, Anal. Bioanal. Chem. 399(9) (2011) 3133-3145. https://doi.org/10.1007/s00216-010-4239-x.

[16] S. Buratti, C. Malegori, S. Benedetti, P. Oliveri, G. Giovanelli, E-nose, e-tongue and e-eye for edible olive oil characterization and shelf life assessment: A powerful data fusion approach, Talanta 182 (2018) 131-141. https://doi.org/10.1016/j.talanta.2018.01.096.

[17] E. Catelli, L. Randeberg, H. Strandberg, B. Alsberg, A. Maris, L. Vikki, Can hyperspectral imaging be used to map corrosion products on outdoor bronze sculptures?, Journal of Spectral Imaging 7(1) (2018) a1. https://doi.org/10.1255/jsi.2018.a10.

[18] G. Guida, M. Marabelli, R. Mazzeo, G. Morigi, Chemical and physical examination of the bronze sculptures of the fountain of Neptune in relation to the restoration, the identification of the construction technique and previous restoration work, Science and technology for cultural heritage (3) (1994) 75-88.

[19] E. Joseph, P. Letardi, R. Mazzeo, S. Prati, M. Vandini, Innovative treatments for the protection of outdoor bronze monuments, Proceedings of the Interim Meeting of the ICOM-CC Metal WG, Amsterdam, Netherlands, 2007, 71-77.

[20] R.J. Barnes, M.S. Dhanoa, S.J. Lister, Standard normal variate transformation and de-trending of near-infrared diffuse reflectance spectra, Appl Spectrosc 43(5) (1989) 772-777. https://doi.org/10.1366/0003702894202201.

[21] P. Oliveri, C. Malegori, R. Simonetti, M. Casale, The impact of signal pre-processing on the final interpretation of analytical outcomes – A tutorial, Anal. Chim. Acta 1058 (2019) 9-17. https://doi.org/10.1016/J.ACA.2018.10.055.

[22] P. Oliveri, C. Malegori, M. Casale, E. Tartacca, G. Salvatori, An innovative multivariate strategy for HSI-NIR images to automatically detect defects in green coffee, Talanta 199 (2019) 270-276. https://doi.org/10.1016/J.TALANTA.2019.02.049.

[23] B. Vekemans, K. Janssens, L. Vincze, A. Aerts, F. Adams, J. Hertogen, Automated Segmentation of μ-XRF Image Sets, X-Ray Spectrom. 26(6) (1997) 333-346. https://doi.org/10.1002/(SICI)1097-4539(199711/12)26:6<333::AID-XRS231>3.0.CO;2-D.

[24] R. Bro, A.K. Smilde, Principal component analysis, Anal. Methods 6 (2014) 2812-2831. https://doi.org/10.1039/C3AY41907J

[25] E. Catelli, G. Sciutto, S. Prati, Y. Jia, R. Mazzeo, Characterization of outdoor bronze monument patinas: the potentialities of near-infrared spectroscopic analysis, Environ. Sci. Pollut. Res. 25(24) (2018) 24379-24393. https://doi.org/10.1007/s11356-018-2483-3.

[26] D.A. Scott, Copper and bronze in art: corrosion, colorants, conservation, Getty publications, Los Angeles, 2002.

CAPTIONS

Figure 1. Sample R57. a) RGB picture – the red rectangle indicates the area submitted to MA-rFTIR mapping analysis. R57 was scanned over an area of 100 by 70 mm²; b) PC1,2,3 score map; c) average spectra extracted from the ROIs; d) ROI 1; e) ROI 2; f) ROI 3. ROI 1 describes the distribution of brochantite, ROI 2 the distribution of Incralac and ROI 3 the distribution of wax applied over the Incralac layer.

Figure 2. Sample R6. a) RGB picture – the red rectangle indicates the area submitted to MA-rFTIR mapping analysis. R6 was scanned over an area of 102 by 65 mm²; b) PC1,2,3 score map; c) average spectra extracted from the ROIs; d) ROI 1; e) ROI 2; f) ROI 3; g) ROI 4. ROI 1 describes the distribution of brochantite, ROI 2 the distribution of a well-preserved Incralac layer, while ROI 3 describes an area with the co-presence of brochantite and Incralac with a higher contribution of brochantite. ROI 4 describes the distribution of wax applied over the Incralac layer.

Figure 3. Detail of the gluteus of the Neptune sculpture. a) RGB picture, the red rectangle indicates the area submitted to MA-rFTIR mapping analysis. The glutes area was 45 by 39 mm²; b) PC1,2,3 score map; c) average spectra extracted from the ROIs; d) ROI 1; e) ROI 2; f) ROI 3. ROI 1 describes an inhomogeneous layer of wax, while ROI 2 describes the co-presence of wax and Incralac with a higher contribution of Incralac. ROI 3 describes a strongly corroded surface in which it is possible to detect the presence of alteration products with some traces of Incralac.

Figure 4. Detail of the shoulder of the Neptune sculpture. a) RGB picture, the red rectangle indicates the area submitted to MA-rFTIR mapping analysis. The shoulder area was 21 by 21 mm²; b) PC1,2,3 score map; c) average spectra extracted from the ROIs; d) ROI 1; e) ROI 2; f) ROI 3; g) ROI 4. ROI 1 and ROI 2 describe the uncleaned area and they are differentiated by a different amount of wax. ROI 3 describes the tape used to limit the untreated area and ROI 4 describes the acetone-cleaned area.

a)

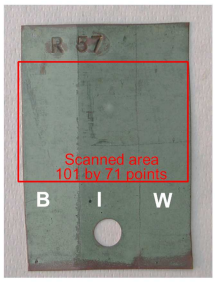

b)

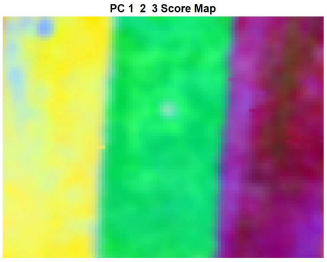

PC	% Expl. Var.	% Cumul. Var.
1	58.4	58.4
2	28.7	87.1
3	5.7	92.8

c)

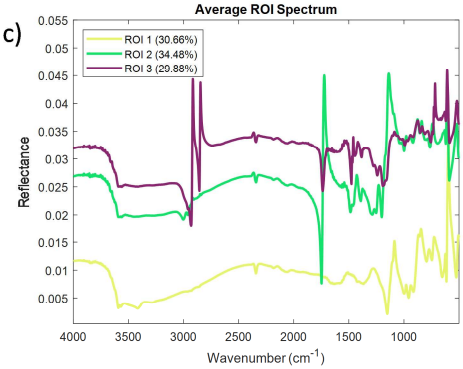

d)

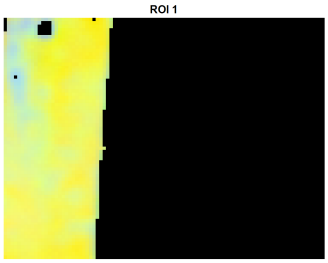

e)

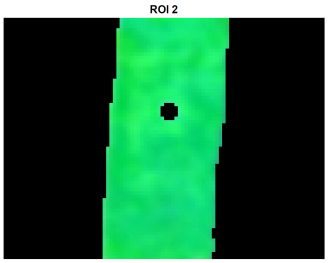

f)

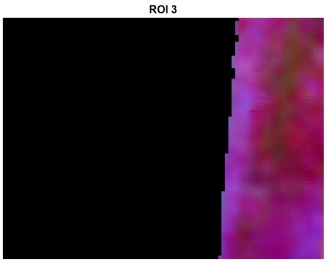

a)

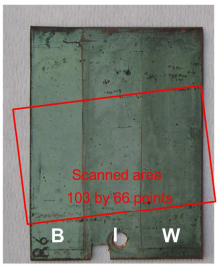

b)

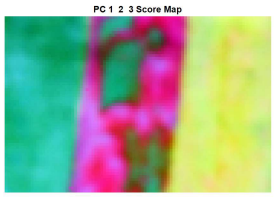

PC	% Expl. Var.	% Cumul. Var.
1	58.3	58.3
2	27.1	85.4
3	5.9	91.3

c)

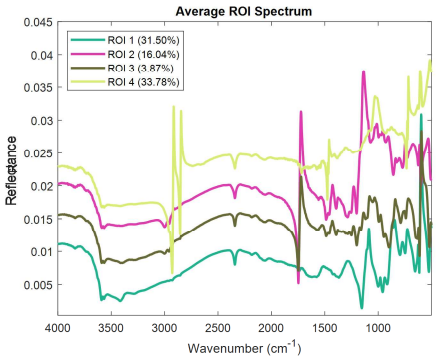

d)

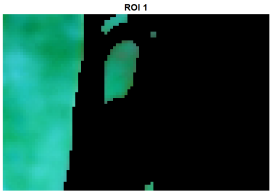

e)

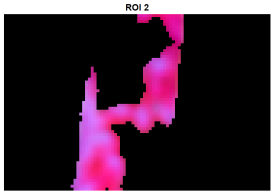

f)

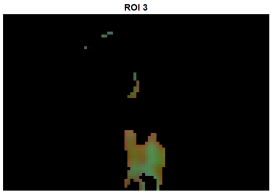

g)

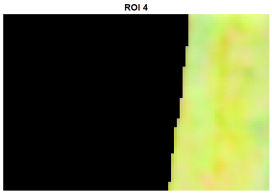

a)

b)

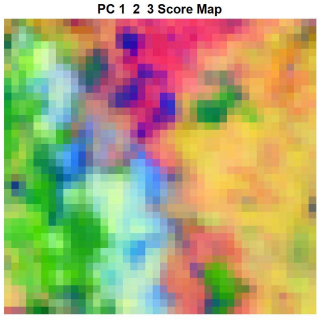

PC	% Expl. Var.	% Cumul. Var.
1	46.9	46.9
2	21.2	68.2
3	11.1	79.3

c)

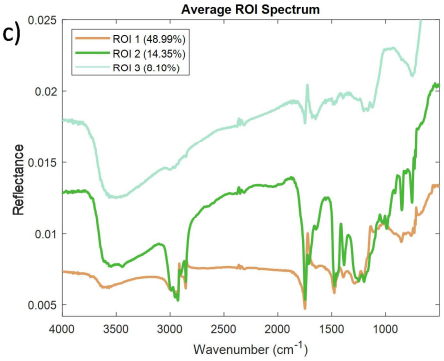

d)

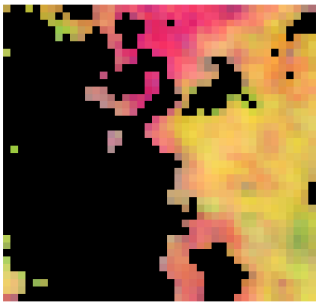

e)

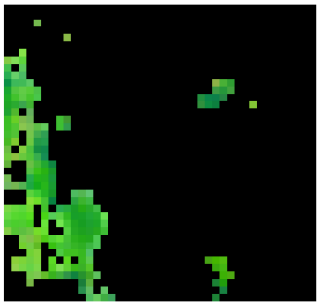

f)

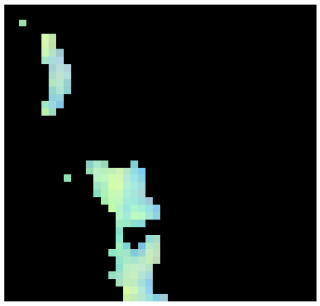

a)

b)

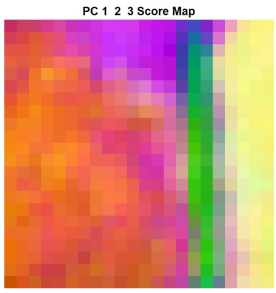

PC	% Expl. Var.	% Cumul. Var.
1	42.1	42.1
2	24.4	66.5
3	7.2	73.7

c)

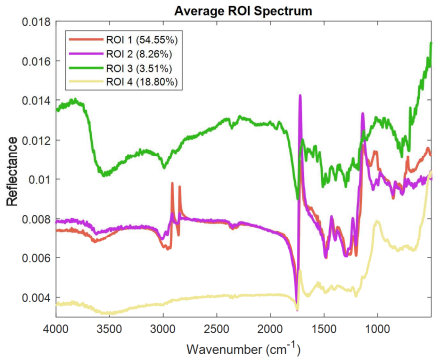

d)

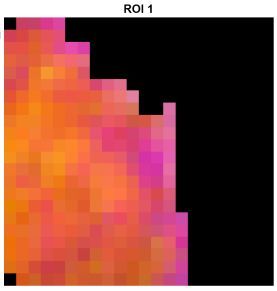

e)

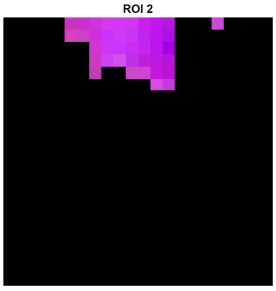

f)

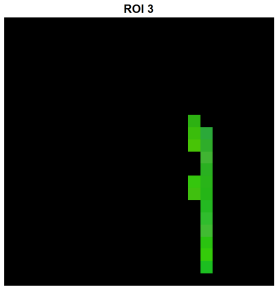

g)

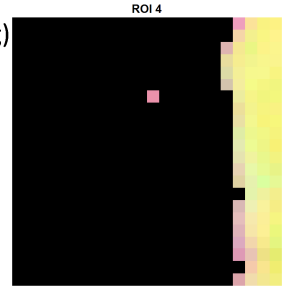

Highlights

1. A new multivariate strategy for automatic on-site processing of hyperspectral data
2. A powerful clustering algorithm (DBSCAN) to automatically identify ROIs
3. Automatic visualization of ROIs and exploratory extraction of average spectra
4. Data analysis is easier and applicable in real time during diagnostic campaigns

Declaration of interests

☒ The authors declare that they have no known competing financial interests or personal relationships that could have appeared to influence the work reported in this paper.

☐The authors declare the following financial interests/personal relationships which may be considered as potential competing interests: